THE MEASUREMENT OF SULFUR OXIDATION PRODUCTS AND THEIR ROLE IN HOMOGENEOUS NUCLEATION

NASA Grant No. NAGW-4692
Georgia Tech Project No. A-5036

056877

Final Report

July 1, 1995 — June 30, 1997

Submitted to:

NASA Headquarters
Washington, DC 20546

Attn: Dr. R. A. Schiffer

Submitted by:

Electro-Optics and Environmental Materials Laboratory
Georgia Tech Research Institute
Georgia Institute of Technology
Atlanta, GA 30332

Principal Investigator: Dr. F. L. Eisele

FINAL REPORT

Work on this project began with a laboratory investigation of ion reaction schemes that would allow the near simultaneous measurement of NH_3, DMSO, and $DMSO_2$ with a single initial reactant ion. If the proper reactant ion could be found, it would make possible fast and sensitive measurements of the above three compounds in remote marine environments, which could add much to our understanding of the DMS oxidation process and the formation of new aerosol particles.

Several different reactant ions have been tested as a possible means for allowing selected ion chemical ionization mass spectrometric (SICIMS) measurements of NH_3, DMSO and $DMSO_2$. All of the tested ions have a sufficiently low proton affinity that they can directly proton exchange with the above 3 compounds of interest. In all but one case, however, their proton affinity is still sufficiently high to minimize reactions with most other atmospheric constituents. Acetone was used to produce $C_3H_7O^+$ ions which will proton exchange with NH_3 to form NH_4^+ for the measurement of ammonia. However, acetone cluster ions $C_3H_7O^+(C_3H_6O)$ also formed rapidly, and do not appear to react quickly with NH_3 thus reducing the attractiveness of using these ions for the above measurements. Protonated DMS was thought to be an attractive reactant ion because DMS can reach concentration of hundreds of ppt in areas where the proposed measurement techniques might be used. If $CH_3SCH_3H^+$ ions were used, enhanced DMS concentrations should have little to no effect on the ion spectrum because the concentration of DMS used to generate the initial DMS reactant ions would be in excess
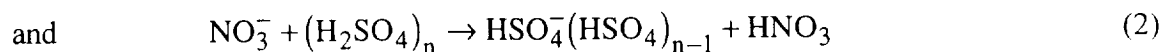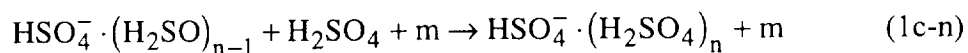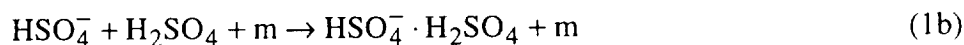
of that present in the atmosphere. It is difficult to find very pure DMS, however, and compounds such as DMSO are common contaminants. Butanol ions were also examined as a possible initial reactant ion for the proposed measurement scheme. There appeared to be some potential contaminants associated with this compound also, but they may not be coming from the original butanol source itself. Thus, this compound needs to be re-examined. The H_3O^+ ion was also examined as a means for measuring NH_3 concentrations. This appeared quite promising for remote marine environments, but a higher proton affinity compound with less potential interferences was still desired.

Protonated ethanol ions were also tested and appear to offer promising new measurement capabilities for a number of compounds. The proton affinity of ethanol is fairly low (188 kcal/mol),[1] so it should react readily with compounds having proton affinities near or above 200 kcal/mol. While it clusters with itself like acetone, the clusters still appear to proton exchange quickly with compounds such as NH_3. Protonated ethanol ions were used in a preliminary continental field study which demonstrated the usefulness of this ion in conjunction with the SICIMS technique for the measurement of gas phase NH_3. This field study will be discussed later in this report.

Much progress has also been made on our nucleation studies. This effort began with the design and construction of a new type of selected ion chemical ionization source: one in which relatively high concentrations of a specific ions could be generated and subsequently injected into a separate drift/reaction region. The drift/reaction region is also

unique in that it allows reaction times to be varied from less than 1 ms to more that 100 ms in an atmospheric pressure gas flow.

This wide range of reaction times is important because it provides a means of separating ion induced molecular cluster formation from ion clusters which result from proton exchange with a pre-existing neutral H_2SO_4 dimer or trimer. In the absence of neutral H_2SO_4 dimers or trimers, $HSO_4^- \cdot (H_2SO_4)_n$ ions (with n > 0) will still form in the presence of gas phase H_2SO_4 by successively incorporating H_2SO_4 molecules onto HSO_4^- ions until some steady state value of n is reached. The latter $HSO_4^-(H_2SO_4)_n$ ions (which will be called ion-induced clusters) are indistinguishable from those resulting from H_2SO_4 dimers or trimers which loose a proton to some initial reactant ion. Thus, $HSO_4^- \cdot (H_2SO_4)_n$ ions which are being used to investigate neutral H_2SO_4 cluster formation have at least two sources:

$$NO_3^- + H_2SO_4 \rightarrow HSO_4^- + HNO_3 \tag{1a}$$

$$HSO_4^- + H_2SO_4 + m \rightarrow HSO_4^- \cdot H_2SO_4 + m \tag{1b}$$

$$HSO_4^- \cdot (H_2SO)_{n-1} + H_2SO_4 + m \rightarrow HSO_4^- \cdot (H_2SO_4)_n + m \tag{1c-n}$$

and $\quad NO_3^- + (H_2SO_4)_n \rightarrow HSO_4^-(HSO_4)_{n-1} + HNO_3 \tag{2}$

Reaction 1 is a multi-step reaction in which the ratio of $\left[HSO_4^- \cdot (H_2SO_4)_{n-1}\right]/\left[HSO_4^-\right]$ is

dependent on $[H_2SO_4]$ and reaction time. In contrast, reaction 2 is simply a proton

exchange reaction between any of the $(HSO_4)_n$ clusters and NO_3^-, and the ratio of

$\left[HSO_4^- \cdot (H_2SO_4)_{n-1}\right]/\left[HSO_4^-\right]$ should not decrease rapidly as reaction time is shortened.

Thus, if the $\left[HSO_4^- \cdot H_2SO_4\right]/\left[HSO_4^-\right]$ ratio is plotted as a function of time for short

reaction times as shown in Figure 1, a linear plot would be expected for the latter ratio if

$HSO_4^- \cdot H_2SO_4$ were formed solely by an ion induced process. Figure 1 shows data

obtained using the recently constructed 1-100 ms ion source/reactor apparatus. The

approximately linear time dependence is expected at the relatively long reaction times

shown, because under such conditions ion-induced cluster formation is known to be

important. At even long times, the ratio of $\left[HSO_4^- \cdot H_2SO_4\right]/\left[HSO_4^-\right]$ must eventually

become time independent at some equilibrium concentration ratio. As the reaction time is

decreased, however, if $(H_2SO_4)_2$ exists and reacts with NO_3^- (which it is expected to),

then the slope of the line in Figure 1 is expected to approach a constant in which the ratio

of $\left[(H_2SO_4)_2\right]/[H_2SO_4]$ is represented by $\left[HSO_4^- \cdot H_2SO_4\right]/\left[HSO_4^-\right]$ times some

relative reaction rate constant for $NO_3^-/(H_2SO_4)_2$ and NO_3^-/H_2SO_4. Therefore much of

our efforts have gone into trying to measure this ratio under near ambient conditions and

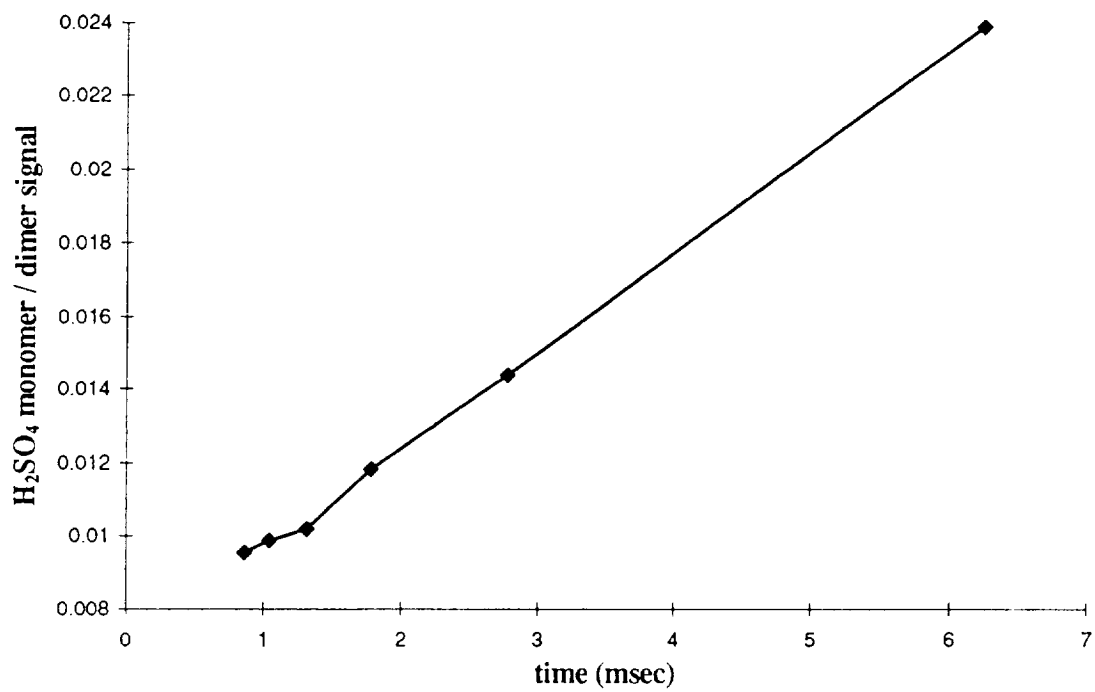at the shortest possible reaction times. The near linear dependence of the ratio (even

Figure 1. Measurement of the ratio of H_2SO_4 monomers to dimer as a function of time at -20°C.

down to the 1 ms time scale) suggests that less than 1% of the gas phase H_2SO_4 molecules are dimers, even at the extreme cases of -20°C and $[H_2SO_4] = 100$ pptv shown in Figure 1. Thus, at temperature and $[H_2SO_4]$ more typical of previous field studies where nucleation events have been observed, the percentage of $(H_2SO_4)_2$ clusters present would probably be expected to be orders of magnitude lower still. While this does not rule out the role of H_2SO_4 dimers and trimers in particle nucleation it does make it seem far less likely that a sufficient number of these clusters exist, and that they will react fast enough with NH_3 to control tropospheric nucleation. As a consequence of these laboratory studies, the most likely tropospheric nucleation mechanism would now appear to be the gas phase reaction of NH_3 with H_2SO_4 (rather than with H_2SO_4 dimers) to form ammonium bisulfate molecules and their subsequent formation of clusters.[2-4] The present study has caused us to reconsider the relevance of a previous experimental laboratory investigation aimed at determining the potential interference of NH_3 in H_2SO_4 measurements. This previous data suggested that while NH_3 does not react quickly with H_2SO_4 in the gas phase, it may, in fact, react slowly. Determining the extent to which NH_3 and H_2SO_4 react to form ammonium bisulfate has, thus, become a central focus of the present study.

A flow tube and injector system has recently been interfaced with the new ion source and SICIMS instrument in an attempt to measure the rate coefficient for the gas phase H_2SO_4/NH_3 reaction. This is an extremely difficult measurement, for several

7

reasons both H_2SO_4 and NH_3 can be rapidly deposited onto the flow tube walls, they can also react with each other on the walls, and the gas phase reaction of interest is expected to be very slow. These measurements are presently under way. We hope to complete them over the next few months and to subsequently look for the molecular cluster products expected from this reaction. This project is divided into two parts because of an administrative fund change at NASA. (While this is a final report for the first portion of this project the overall research project itself is expected to continue for an additional year as originally proposed. It is during this final year that the latter reaction would be studied.)

Other areas of progress include measurements of the accommodation coefficient of H_2SO_4 on ammonium sulfate, sodium chloride and other particles surfaces. These measurements were made in our laboratory in conjunction with colleagues from the University of Minnesota. The accommodation coefficient for H_2SO_4 is important not only for understanding the growth of CN into CCN, but it is also used to calculate the flux of nucleating particles from measured ultrafine particle distributions. Since literature values of this coefficient vary by nearly 2 orders of magnitude (0.02-1.0), and we had the ability to make the first direct measurement of these parameters, it seemed like a worthwhile project. The accommodation coefficients were found to be 0.73 ± 0.21 and 0.80 ± 0.23 for ammonium sulfate and sodium chloride respectively. The details of this very successful measurement have recently been published and a copy of the paper is included as Appendix A.

Progress has also been made on testing new ion reaction schemes for measuring NH_3 in the field. In the first year of this grant, several ions were tested in the laboratory as possible candidates for the reactant ion to be used for measuring NH_3 in the atmosphere. This year, an approximately 1 month long local field study was conducted, in which two reactant ions were tested for use in measurements of ambient NH_3 and various hydrocarbons by SICIMS. One of the compounds tested was acetone, which was previously used in some of the past year's laboratory tests. A second compound used to generate reactant ions was ethanol, and the latter results look very encouraging. Both compounds readily form ions by attaching a proton, and both also readily form clusters with themselves. In the case of ethanol the most common cluster ion $C_2H_7O^+ \cdot C_2H_6O$ still appears to react quickly with NH_3 via proton exchange to form NH_4^+ and $NH_4^+ \cdot C_2H_6O$. Figure 2 shows the initial ethanol reactant ion distribution in ambient air which is dominated by $C_2H_7O^+ \cdot C_2H_6O$, but which also contains a small peak of the core ion $C_2H_7O^+$. The NH_4^+ and $NH_4^+ \cdot C_2H_6O$ peaks are a result of reactions of $C_2H_7O^+ \cdot (C_2H_6O)_n$ for n=0,1 with ambient NH_3 at a field site a few km north of the NCAR Mesa Laboratory Building at the edge of the foothills of the Rocky Mountains. Air flow at this site is typically from the west and is relatively clean during the morning hours. At some point during late morning or early afternoon, the flow will typically switch to a more easterly (or sometimes northerly and southerly) component, which brings up air from the city of Boulder, Denver, or farming areas to the east. Figures 2 and 3 show a measured ion spectrum and an initial test of the new SICIMS ammonia

Ambient Spectra December 30, 1996

NH_4^+ = Ammonia + H^+
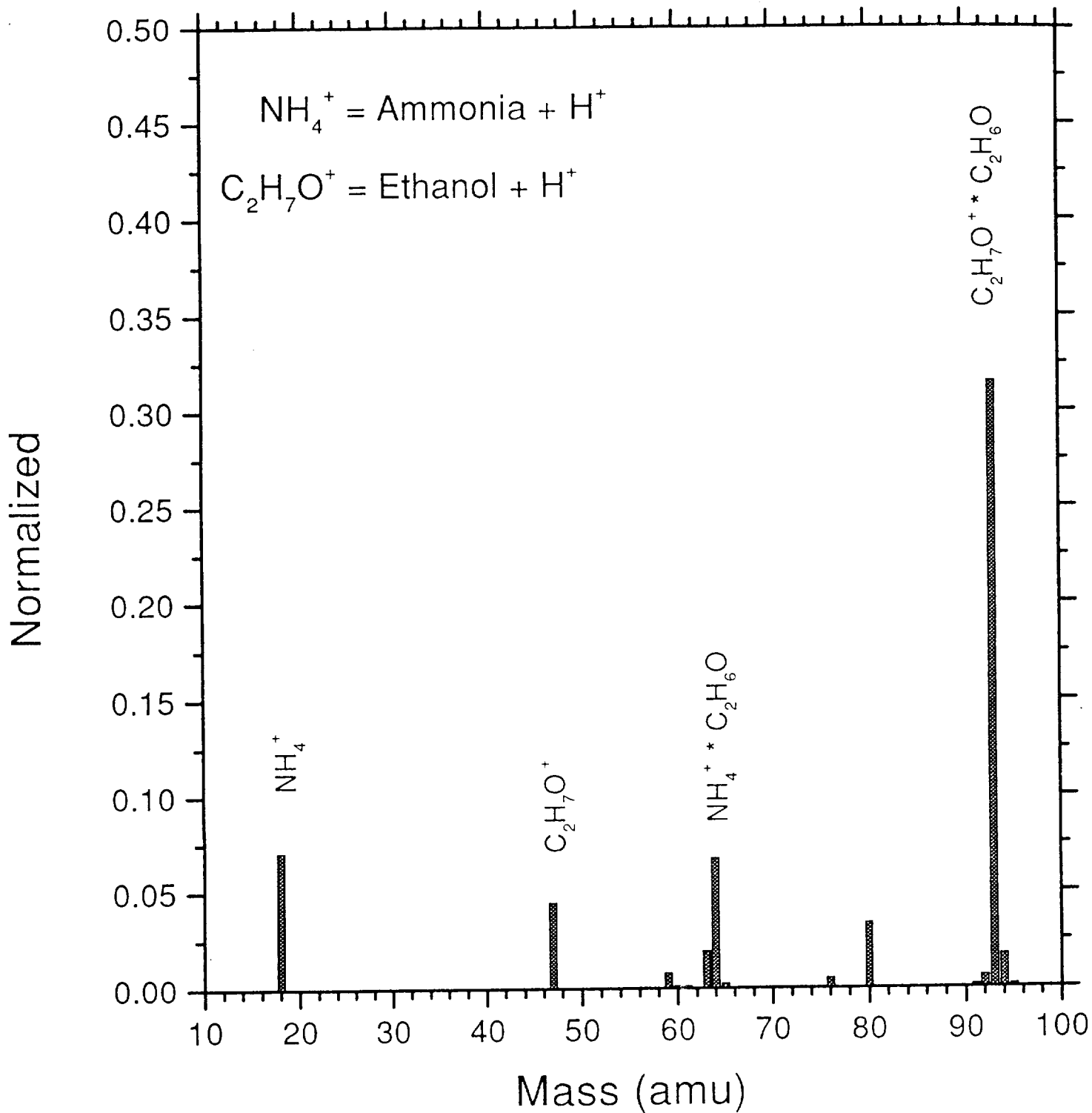
$C_2H_7O^+$ = Ethanol + H^+

Figure 2. Typical ion spectrum measured during a recent field study showing nearly exclusively reactant and production peaks.
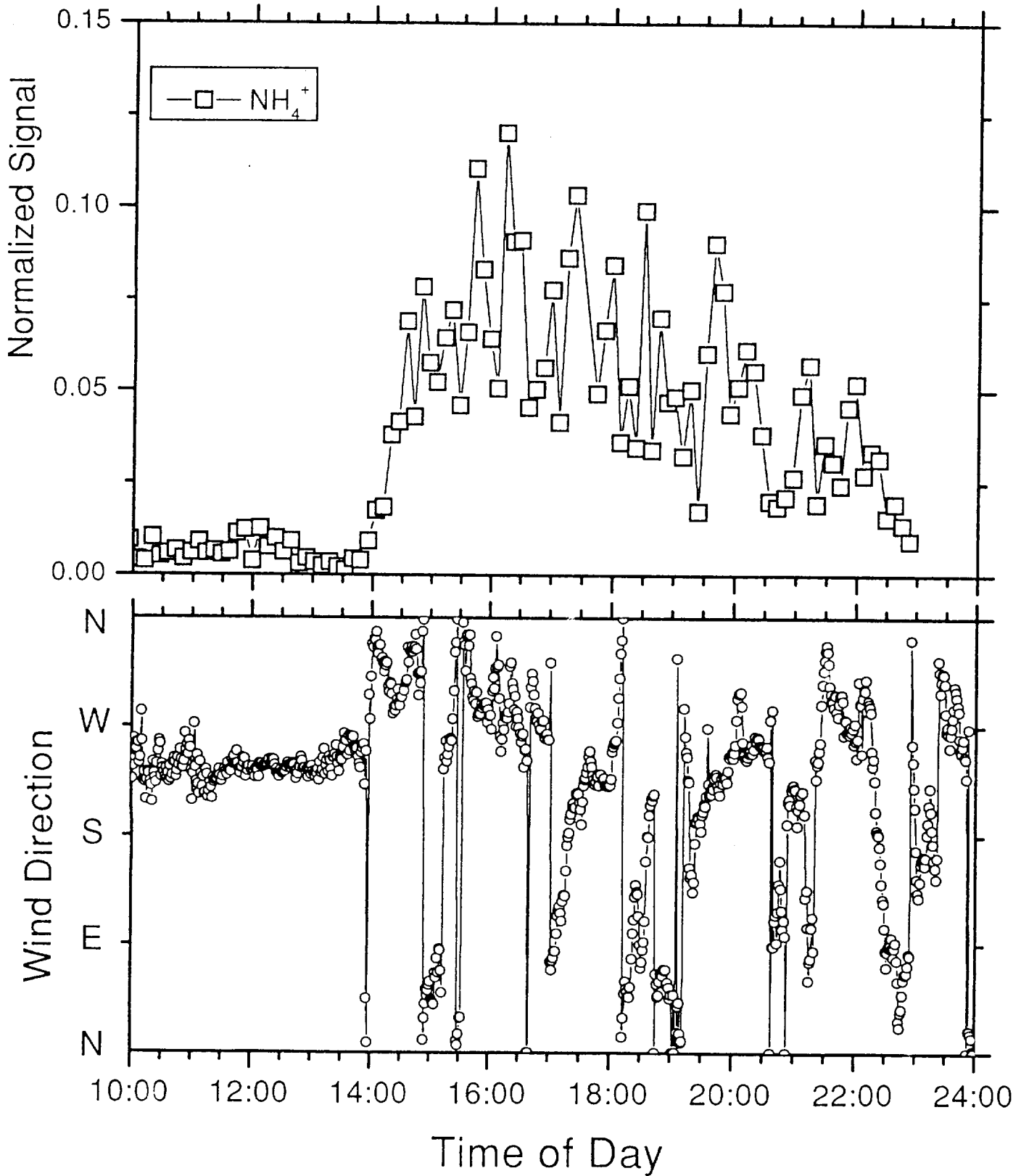
December 30, 1996

Figure 3. Preliminary measurements of NH_3 and wind direction as a function time of day.

measurement technique used at this site. Figure 3 also shows the wind direction during this same time period. As is typical of this site, prevailing westerlies bring down relatively clean air from the mountains which, as seen from Figure 3, contains little NH_3. In early afternoon at about 14:00 hours, the wind switches direction abruptly and its velocity drops. The air mass present after 14:00 is probably from urban and farm areas and would be expected to contain far more NH_3, which agrees well with the observations shown in Figure 3. Thus far, only very preliminary tests of this new technique have been performed, but the results look quite promising, particularly since the area in which these measurements were made contains large amounts of hydrocarbons which could have had a much larger than observed interference. For measurements in marine environments, $C_2H_7O^+$ can probably be used to measure NH_3, and DMSO with the same ion source.

The present development and testing of new SICIMS measurement schemes is also expected to continue throughout the next year. While ions such as $C_2H_7O^+$ show much promise for making measurements of compounds such as NH_3, and DMSO, it is quite possible that DMS and $DMSO_2$ can also be measured with the same ion source. Thus, these and similar reaction schemes for other DMS oxidation products will continue to be a major focus of the second phase of this study.

References

1. Lias, S.G., J.F. Liebman, and R.D. Levin, Evaluated gas phase basicities and proton affinities of molecules; heats of formation of protonated molecules, *J. Phys. Chem. Ref. Data, 13*, 695, 1984.

2. Eisele, F.L., and P.H. McMurry, Recent progress in understanding particle nucleation and growth, *Phil. Trans. R. Soc. Lon., B352*, 191, 1997.

3. Weber, R.J., J.J. Marti, P.H. McMurry, F.L. Eisele, D.J. Tanner, and A. Jefferson, Measured atmospheric new particle formation rates: Implications for nucleation theory, *Chem. Eng. Comm., 151*, 53, 1996.

4. Marti, J.J., A. Jefferson, X. Ping Cai, C. Richert, P.H. McMurry, and F. Eisele, H_2SO_4 vapor pressure of sulfuric acid and ammonium sulfate solutions, *J. Geophys. Res., 102*, 3725-3735, 1997.

Measurements of the H_2SO_4 mass accommodation coefficient onto polydisperse aerosol

A. Jefferson,[1] F. L. Eisele,[1,2] P. J. Ziemann,[3] R. J. Weber,[4] J. J. Marti,[5] and P. H. McMurry[6]

Abstract. The loss rate of H_2SO_4 vapor onto submicron particles was measured for three different particle substrates. The experimental technique involved direct flow tube measurements of H_2SO_4 decay rates onto a polydisperse aerosol using chemical ionization mass spectroscopic detection. The aerosols of this study were partially hydrated crystalline salts with diameters in the size range of 20 to 400 nm. The mass accommodation coefficients, α, were calculated from the first-order rate constants for H_2SO_4 loss to be 0.73 ± 0.21 and 0.79 ± 0.23 for loss onto $(NH_4)_2SO_4$ and NaCl, respectively. Measurements of the loss rate of H_2SO_4 onto a NaCl aerosol coated with stearic acid resulted in lower mass accommodation coefficients with values of 0.31 and 0.19 for aerosol with high and low stearic acid coverage, respectively. The observed decrease in α on an aerosol with a hydrocarbon coating suggests that aerosol composition is a key factor in H_2SO_4 adsorption on to a particle surface.

Introduction

Aerosols have a significant impact on climate forcing by their ability to scatter solar radiation and increase cloud albedo, which result in a cooling of the lower troposphere [Penner et al., 1997; Wigley and Raper, 1992]. The magnitude of this effect depends in part on the aerosol microphysical properties, particularly the particle composition, size, and number density [Schwartz, 1996]. Sulfates, along with nitrates and organics, form the primary constituents of submicron condensation nuclei (CN), which scatter shortwave radiation and can grow to form cloud droplets. The formation and initial growth of CN are thought to proceed through bimolecular nucleation of H_2O and H_2SO_4 and subsequent uptake of gas phase H_2SO_4 onto the particle surface [Kriedenweis et al., 1991]. An unknown parameter needed to quantify CN nucleation and growth rates is the mass accommodation coefficient of H_2SO_4 onto particles.

Current models of aerosol nucleation rates are especially sensitive to the H_2SO_4 mass accommodation coefficient, α. Estimates of α range between 0.02 and 1.0. In their model of bimolecular nucleation rates, Pandis et al. [1994] calculated a 45% reduction in the H_2SO_4-H_2O nucleation rate when α was changed from 0.02 to 0.05. Nucleation rates modeled by Kulmala et al. [1995] show a similar strong dependence on α.

In laboratory measurements of aqueous H_2SO_4 particle growth, Van Dingenen and Raes [1991] determined a value for α between 0.02 and 0.09. Alternatively, two field studies, which measured steady state H_2SO_4 production rates [Eisele and Tanner, 1993; Weber et al., 1997], found that values for α of 0.5 and 1.0, respectively, gave good agreement with their data.

Submicron aerosol composition may vary between remote or polluted and marine or continental environments. Aerosols from remote marine environments were found to contain mostly SO_4^{2-}, $CH_3SO_3^-$, and NH_4^+ ions, while larger sea salt aerosols also contain Na^+ and Cl^- ions [Huebert et al., 1996; Savoie et al., 1993]. In addition, aerosols found in continental and anthropogenically influenced air masses may contain considerable amounts of organics [Saxena and Hildemann, 1996; Novakov and Penner, 1993]. As the substrate composition varies, so too may the uptake of H_2SO_4. As an acid, H_2SO_4 would seem likely to bond most strongly with substrates containing polar or basic binding sites.

Here we present measurements of the mass accommodation coefficient of H_2SO_4 onto aerosols composed of $(NH_4)_2SO_4$, NaCl, and NaCl coated with stearic acid. This study is the first measurement of the gas phase H_2SO_4 uptake rate onto aerosols that directly measured changes in the gas phase H_2SO_4 concentration. The aerosol uptake experiments in this study use the sensitive technique of selected ion chemical ionization mass spectrometry (SI/CIMS) to measure the removal rate of H_2SO_4 by aerosols. In this study, H_2SO_4 concentrations in the range of 0.1-10 parts per trillion by volume were measured at a relative humidity at or below 11%. Measurements at a higher relative humidity, representative of the lower troposphere, were hindered by the low equilibrium vapor pressure of H_2SO_4 above the acid solution source used in these experiments. Possible changes in the H_2SO_4 mass accommodation coefficient with ambient conditions such as relative humidity and aerosol composition are discussed.

[1]Atmospheric Chemistry Division, National Center for Atmospheric Research, Boulder, Colorado.

[2]Also at Georgia Research Institute, Georgia Institute of Technology, Atlanta.

[3]Statewide Air Pollution Research Center and Department of Soil and Environmental Sciences, Unversity of California, Riverside.

[4]Environmental Sciences Laboratory, Brookhaven National Laboratory, U.S. Department of Energy, Upton, New York.

[5]Computational Physics, Inc., Fairfax, Virginia.

[6]Particle Technology Laboratory, Department of Mechanical Engineering, University of Minnesota, Minneapolis.

Experimental Method

Polydisperse aerosols were generated by atomizing aqueous solutions of either $(NH_4)_2SO_4$ or NaCl. Filtered

nitrogen was used as a carrier gas for the aerosol flow at a flow rate of about 1.24 L min⁻¹. The aerosol droplets passed through a silica gel diffusion dryer before joining the humidified nitrogen carrier flow at the entrance of the flow tube injector. Particle sizes ranged in diameter from 20 to 400 nm. In the experiments involving stearic acid coated aerosols, NaCl particles were coated with stearic acid by passing the aerosol flow through a heated 6 inch long glass tube containing both solid stearic acid and its vapor. The thickness of the acid coating on the particles was controlled by adjusting the temperature of the glass tube and thus the stearic acid vapor pressure. The tube was heated to 104° and 88°C for high and low particle coatings of stearic acid, respectively. The aerosol flow made up about 5% of the total gas flow.

Aerosol surface areas were determined from particle size distributions measured by using a scanning electrical mobility spectrometer (SEMS) [*Wang and Flagan*, 1990]. The instrument consists of a particle charger, a differential mobility analyzer (DMA), a condensation nucleus counter (CNC), and SEMS software for rapid scanning of the particle size distribution. Sampled particles were charged to near-Boltzmann equilibrium by a ²¹⁰Po source. The particles then passed through a DMA, which separated particles by their electrical mobility, allowing only those with mobilities in a narrow selected range to exit to the CNC detector. The particle mobility distribution was measured by scanning through the particle size range, typically 20 nm to 400 nm in diameter. For spherical particles, whose size is precisely defined by the diameter, the particle size distribution can be accurately calculated from the mobility distribution.

In our experiments, aerosol was sampled from the downstream end of the flow tube reactor and diluted with filtered, dry nitrogen (~1:6) in order to maintain particle concentrations in the instrument range. The aerosol flow rate into and out of the DMA was 1.0 L min⁻¹, the DMA sheath air flow rate was 7.3 L min⁻¹ of filtered room air, and the CNC flow rate was 1.5 L min⁻¹, of which 1.0 L min⁻¹ was aerosol from the DMA, the remainder being filtered room air. The use of filtered room air for the DMA sheath flow should have no effect on the measured particle size distribution, since the ambient relative humidity was well below the deliquescence point of both NaCl and (NH₄)₂SO₄.

The particle size distributions used for our calculations of aerosol surface areas were corrected for particle charging and losses in the DMA by using the method of *Hagan and Alofs* [1983]. No correction for CNC counting efficiency was required, since the aerosol surface area was associated with sizes that are detected with near 100% efficiency. The flow was laminar in the flow tube and the tube leading to the DMA, making particle losses by diffusion negligible. Aerosol surface areas were calculated by assuming that the particles were spherical, which is approximately true for (NH₄)₂SO₄ [*Kelly and McMurry*, 1992] although not for NaCl. Nonetheless, because NaCl particles are apparently cubic [*Lodge and Tufts*, 1955] and the ratio of the side length of a cube to its mobility diameter is 0.746 [*Dahneke*, 1973], the surface area for a sphere and a cube with the same mobility diameters differ only by ~6%. Typical aerosol surface areas per cubic centimeter for these experiments were 600 μm² cm⁻³.

Flow Tube Apparatus

The reaction tube for measurement of kinetic decay rates consisted of a jacketed Pyrex flow tube, 80 cm in length with a

7.6 cm inside diameter. A movable, 2.5 cm diameter Pyrex injector was mounted inside the flow tube. The injector diameter reduces to a small orifice about 5 cm before its exit. After this constriction the injector flares to nearly the full diameter of the flow tube and has a stainless steel, fine mesh screen attached on the end. The H₂SO₄ vapor source consisted of a small cap containing a concentrated H₂SO₄ solution which rested on top of the injector end screen. The injector design ensured that the aerosol flow turbulently mixed with H₂SO₄ vapor in this region between the constriction and injector exit and that the total gas flow was evenly distributed across the flow tube diameter. A schematic diagram of the experimental setup is given in Figure 1.

The H₂SO₄ concentration in the flow gas depended on the equilibrium vapor pressure of H₂SO₄ above the acid solution source and thus varied strongly with the relative humidity of the gas flow. At relative humidities above 10% the H₂SO₄ vapor pressures of sulfuric acid solutions drop below 10⁻⁹ torr [*Ayers et al.*, 1980; *Marti et al.*, 1997], which resulted in H₂SO₄ concentrations too low to measure an accurate decay. The present measurements were limited to a relative humidity between 11% and 0.3%.

The temperatures of both the flow tube and the humidified carrier gas were maintained at a constant 25°C. A humidified airstream was generated by flowing N₂ gas through microporous polytetrafluoroethylene (PTFE) tubing immersed in deionized and distilled water. This airstream then flowed through a heat exchanger before combining with the aerosol flow in the injector tube entrance. Water from a temperature-controlled bath was circulated through both the external flow tube jacket and the gas heat exchanger. The gas temperature was measured by a thermocouple at the flow tube exit. The relative humidity of the carrier gas was measured at the flow tube exit by a dew point monitor.
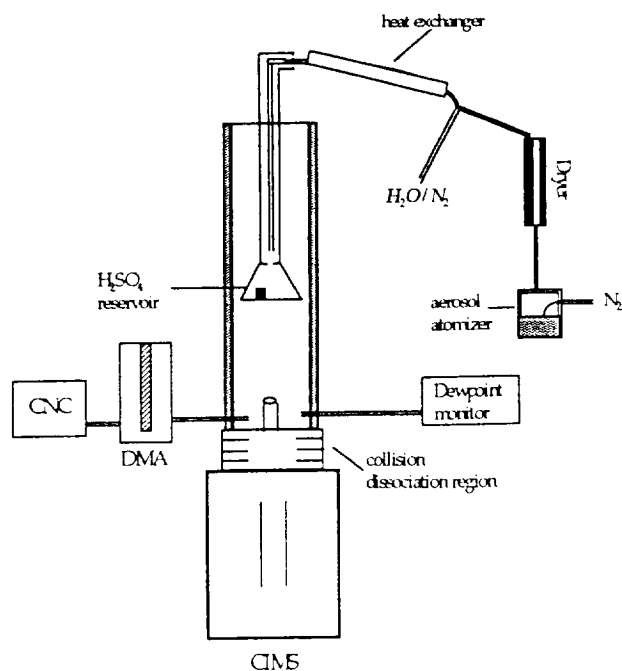

Figure 1. Diagram of flow tube kinetic reaction cell, aerosol generation and detection, and CIMS instrument.

CIMS Detection of H₂SO₄

The decay in the H₂SO₄ concentration as a function of injector position was measured by SI/CIMS. This technique involved sampling the gas from the center of the flow tube into a chemical ionization source. After merging with the ions from this source, the gas flowed through a reaction region, where H₂SO₄ in the flow gas underwent a proton exchange reaction with NO_3^- and was converted to HSO_4^-. The reactant and product ions were then focused into a mass spectrometer and detected. The relative H₂SO₄ concentration is given as the ratio of the HSO_4^-/NO_3^- ion signals. Two steps were taken to assure that hydrates of H₂SO₄ were detected along with the monomer. Before entering the mass spectrometer the ion-containing gas was directed through a flow of dry nitrogen gas, which acted to dehydrate the ions. Next the ions passed through a small aperture into a collision dissociation region. A voltage held across the vacuum chamber accelerated the ions and induced collisions with the background nitrogen gas strong enough to dissociate any remaining ion clusters. Thus hydrates of HSO_4^- were converted to the monomer sulfate ion and detected with the same efficiency. Further details of the CIMS instrument can be found in prior publications [*Eisele and Tanner*, 1991, 1993; *Tanner and Eisele*, 1995; *Tanner et al.*, 1996].

Flow Time Measurements

At a flow rate of 23.5 L min⁻¹ and a Reynolds number of 650 typical of the present experiment, the gas in the flow tube shown in Figure 1 is expected to develop a laminar flow profile with some radial and axial diffusion. However, to promote a short ion-molecule reaction time, the flow in the CIMS sample inlet was considerably faster than that in the main flow tube, and as a result the flow accelerated, permitting a radial convergence of the gas in the flow tube into the sample inlet. Only a central portion of the full flow tube was sampled. Rather than assume laminar flow conditions, we measured the flow time directly, using a pulsed ion source. A corona discharge ion source was constructed by running a wire down the center of the injector to a distance within 2-3 cm of the end metal screen, which was held at electrical ground so that the flow tube remained a near field free region. A counter card triggered a 5 kV, 10 ms wide electrical pulse to induce the corona discharge and also initiate computer data collection. Data was collected in 10 s cycles with 0.2 s time steps. The flow times were calculated by using a weighted average of the signal counts at each time step are best fit by the equation

$$\text{time (in seconds)} = 0.0639x + 0.3715 \qquad (1)$$

where x is the injector position in centimeters from the top of the CIMS sample inlet tube.

Unlike a neutral gas, a positively charged ion flow is subject to space charge repulsions, which accelerate the ions, thereby increasing the diffusivity of the ions beyond that of neutral molecules. Increased ion diffusivity results in a broader time profile and shifts the measured residence time of the ion to times longer than those of the neutral molecule. Under the flow conditions of these experiments the CIMS instrument sampled about 18% of the flow tube area. An ideal laminar flow with no radial or axial diffusion would result in a flow rate, averaged over a central cross section of the flow

tube, of time (in seconds) $= 0.0616x$. The difference between this flow rate and the measured value of $0.0639x$ given in equation (1) is due to diffusional broadening of the time profile. The time offset of 0.3715 s in equation (1) reflects the time needed for the ions to travel from a relative zero position on the flow tube to registering an ion signal on the computer. The small difference in the ideal laminar flow rate and the measured ionic flow rate indicates that the difference between the radial and axial diffusion of the ions and neutral molecules is small for the low ion concentrations of these experiments and has a negligible effect on the measured flow times. The exponential fits of the experimental decays used a value for the reaction time given by equation (1).

Reaction Kinetics and Mass Transport

The loss of H₂SO₄ onto an aerosol surface follows pseudo first-order kinetics, provided the aerosol number density and uptake ability remain constant during the course of a single measurement. Changes in the H₂SO₄ concentration with injector position can be expressed as in the following equation;

$$\frac{d[H_2SO_4]}{dt} = -K[H_2SO_4] + k_{re}[H_2SO_4]_s \qquad (2)$$

Here, $K = k_1 + k_d$, where k_1 is the pseudo first-order rate constant for loss of H₂SO₄ onto aerosol and k_d is the background decay constant for diffusion and wall losses of H₂SO₄. The variable k_{re} is the rate constant for reevaporation of H₂SO₄ from the aerosol surface, and $[H_2SO_4]_s$ is the aerosol surface concentration of H₂SO₄.

Previous measurements by *Marti et al.* [1997] of the H₂SO₄ vapor pressure above $(NH_4)_2SO_4$ aerosols indicate that the evaporation rate of H₂SO₄ from the aerosol is quite small, producing an H₂SO₄ concentration of the order of 10^4 molecules cm⁻³, below detection limit of these experiments. H₂SO₄ coverage of the aerosol surface over the duration of the longest decay times was less than 1% of the total aerosol surface area. Because of the low H₂SO₄ surface coverage and low H₂SO₄ vapor pressure above $(NH_4)_2SO_4$ aerosols, reevaporation of H₂SO₄ from both $(NH_4)_2SO_4$ and NaCl aerosols was considered negligible, and the second term in equation (2) was set equal to zero.

A determination of k_1 will depend on the mass transport between H₂SO₄ and the particles. The particles generated in these experiments are between 20 and 400 nm in diameter and fall in the transition regime between gas kinetic and diffusion limits for mass transport. For uptake onto a monodisperse aerosol the first-order rate constant can be calculated in terms of a mass accommodation coefficient, α, with the Fuchs-Sutugin equation [*Fuchs and Sutugin*, 1970]

$$k_1 = \frac{\alpha N_p c \pi D^2}{4(1 + \alpha B)} \qquad (3)$$

where

$$B = \frac{(0.75 + 0.283Kn)}{Kn(Kn + 1)} \qquad (4)$$

From the above, N_p is the particle number density, c is the mean molecular speed, D is the particle diameter, and Kn is the

Knudsen number, which is a function of the molecular diffusivity, D_g, and particle size: $Kn = 6D_g/cD$. Here the mass accommodation coefficient represents the number of H$_2$SO$_4$ molecules reversibly adsorbed onto the particle surface per gas kinetic collision.

For a polydisperse aerosol distribution the observed k_1 is the integral with respect to the particle diameter, D, of the size dependent pseudo first-order rate constant for H$_2$SO$_4$ loss on the aerosol, i.e.,

$$k_1 = \int k_1(D)dD \qquad (5)$$

Numerically integrating over D, we obtain the following equation:

$$k_1 = \sum_i \frac{\alpha c \pi D_i^2 \dfrac{dN}{d\ln D_i}}{4(1 + \alpha B_i)} \Delta \ln D_i \qquad (6)$$

The aerosol number concentration for each particle diameter, $(dN/d\ln D)\Delta \ln D$, was calculated as an average of all of the size distributions recorded at various injector positions for a given decay. Calculation of the mass accommodation coefficient involved iteratively changing α in the equation for k_1 until the calculated value of k_1 equaled the measured value.

The diffusion coefficient, D_g, of H$_2$SO$_4$ in N$_2$ was chosen to be 0.1 ± 0.02 cm^2 s^{-1} in accordance with prior calculations [Roedel, 1979; Marti et al., 1997] and adjusted for an ambient pressure of 615 torr. In a humid airflow a fraction of the H$_2$SO$_4$ molecules are hydrated and have a lower effective diffusivity. However, at the low relative humidities of these experiments, most of the H$_2$SO$_4$ molecules were unhydrated or monohydrated. The small decrease in diffusivity of the monohydrate relative to H$_2$SO$_4$ is expected to be well within the uncertainty in the value of D_g [Marti et al., 1997].

Results

The first-order decay of H$_2$SO$_4$ onto an aerosol surface was measured for submicron polydisperse particles composed of (NH$_4$)$_2$SO$_4$, NaCl, and NaCl coated with stearic acid. Figure 2 shows the H$_2$SO$_4$ signal versus injector position for different concentrations of NaCl aerosol. The measured first-order rate constants and calculated values of the mass accommodation coefficient along with the uncertainties are given in Table 1 for H$_2$SO$_4$ loss onto each of the substrates. The mass accommodation coefficients for H$_2$SO$_4$ loss onto (NH$_4$)$_2$SO$_4$ and NaCl aerosol were found to be 0.73 ± 0.21 and 0.79 ± 0.23, respectively. The measurement uncertainties are given as 2σ, twice the standard error for each set of measurements. The measured mass accommodation coefficients for H$_2$SO$_4$ uptake onto NaCl particles coated with stearic acid had an average value of 0.25, indicating a significantly lower loss rate for H$_2$SO$_4$ onto an aerosol with a hydrocarbon film.

The mass accommodation coefficients measured for H$_2$SO$_4$ loss onto NaCl and (NH$_4$)$_2$SO$_4$ aerosol in this study are similar and fall within the uncertainty range of either measured value. The relative humidity of the flow gas in these experiments was well below the deliquescence point of both salts, so that the uptake likely represents a physical adsorption of H$_2$SO$_4$ onto a partially hydrated crystalline salt surface [Ewing and Peters, 1997]. The similarity in the two surfaces with respect to H$_2$SO$_4$ adsorption is evident from the small difference in α for the salts.

The value of α found for a NaCl aerosol coated with stearic acid was approximately a factor of 3 smaller than that measured for the bare aerosol. Stearic acid is a long-chain carboxylic acid (CH$_3$(CH$_2$)$_{16}$COOH) that is insoluble in water and consequently is expected to form a film on the aerosol surface. Figure 3 shows the aerosol size distribution for bare NaCl particles and NaCl particles with thick and thin coatings of stearic acid. The aerosol with the higher coverage
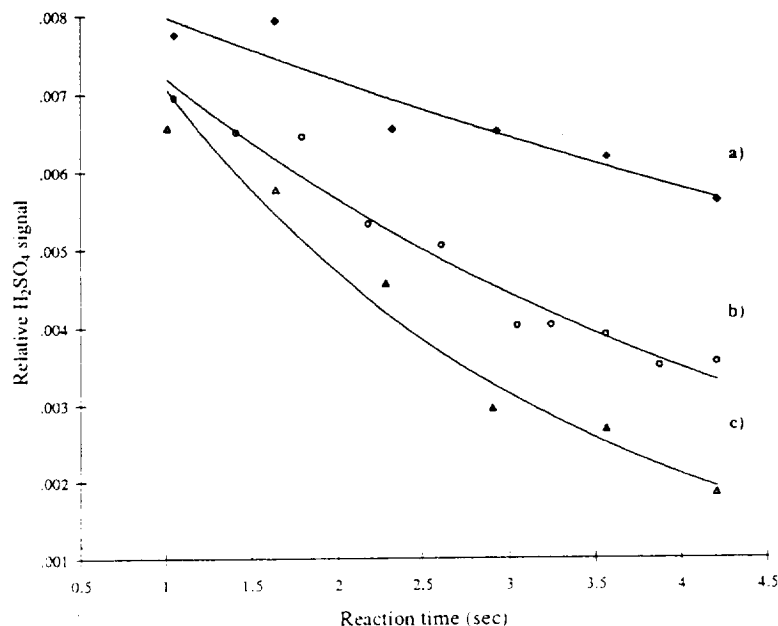

Figure 2. Relative H$_2$SO$_4$ signal versus injector position under conditions of (a) no aerosol present, (b) an aerosol surface area of 3.0×10^{-6} cm^2 cm^{-3}, and (c) an aerosol surface area of 8.8×10^{-6} cm^2 cm^{-3}.

Table 1. Summary of Measured First-Order Rate Constants (k_1), Diffusional and Wall Loss Constant (k_d), and Mass Accommodation Coefficients (α)

RH, %	k_1,s^{-1}	k_d,s^{-1}	α	Uncertainty
		NaCl		
1.6	0.378	0.120	0.62	0.20
0.3	0.139	0.093	0.85	0.30
1.7	0.136	0.108	0.78	0.25
1.4	0.169	0.098	0.91	0.34
11.0	0.391	0.048	0.91	0.26
5.2	0.341	0.066	0.70	0.21
		(NH$_4$)$_2$SO$_4$		
1.9	0.383	0.109	0.75	0.22
5.2	0.327	0.066	0.80	0.26
0.5	0.250	0.122	0.64	0.37
		Stearic Acid		
5.4	0.241	0.074	0.31	0.08
4.4	0.086	0.089	0.19	0.06

RH, relative humidity.

of stearic acid resulted in a faster loss rate of H$_2$SO$_4$ and thus a larger value for α; α = 0.31 and 0.19 for high and low stearic acid coverage, respectively. This difference between high and low coverage could be due to a change in the orientation of the acid on the aerosol surface, leading to a concomitant change in the number of polar binding sites available for H$_2$SO$_4$. Alternatively, the aerosol surface with the higher stearic acid coverage may have been highly irregular, resulting in a higher aerosol surface area. In the high-coverage experiments the appearance of a shoulder at large particle diameters in the particle size distribution may indicate the presence of stearic acid aerosols in addition to the coated salt aerosols. The shape of stearic acid aerosols may be even more irregular than that of the coated aerosols and can lead to an underestimate of the total aerosol surface area. Certainly, more knowledge of the aerosol surface structure and a far more

extensive set of uptake measurements are needed to understand H$_2$SO$_4$ loss rate onto aerosols containing organics.

Discussion of Error

Error in the calculated value of α will arise from uncertainty in the diffusion coefficient, point to point variation in the aerosol surface area during a single decay, uncertainty in the measured aerosol surface area, and changes in the H$_2$SO$_4$ vapor pressure with instabilities in the flow gas relative humidity. Changes in the value of D_g of ±20% lead to only a 3% change in α. An uncertainty in α near 5% could be accounted for from the standard deviation in the averaged aerosol size distributions within a single experimental decay measurement. In contrast, the H$_2$SO$_4$ vapor pressure above the solution source was very sensitive to changes in the relative
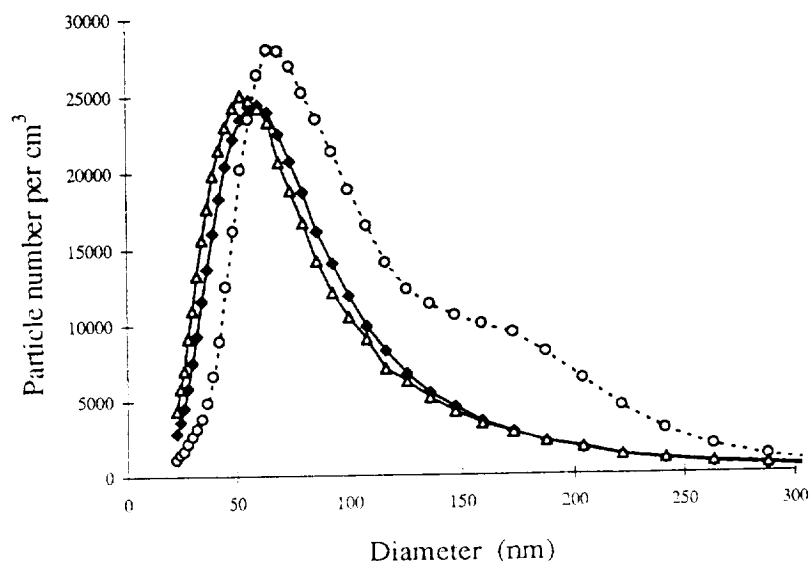

Figure 3. NaCl aerosol size distributions with no stearic acid (triangles), low stearic acid (diamonds), and high stearic acid coverage (circles).

humidity, which added to the uncertainty in the observed first-order rate constant and mass accommodation coefficient. The vapor pressure of H$_2$SO$_4$ above a solution declines exponentially with increased relative humidity [Marti et al., 1997; Ayers et al., 1980]. In the dry flow gases of these experiments, a 0.1% change in the relative humidity (RH) in the flow gas from 1 to 1.1% could produce a change in the H$_2$SO$_4$ vapor pressure of the order of 3×10^7 molecules cm^{-3}, i.e., close to 15% of the concentration range of the signal decay. The H$_2$SO$_4$ signal was far less sensitive to changes in the water vapor pressure at a relative humidity above 5%. Error arising from small variations in the flow gas relative humidity and aerosol size distribution is evident in the calculated fit of the signal to an exponential decay. As can be seen from Table 1, the uncertainties in the calculated values of α are highest in the decays with the lowest relative humidity.

As a result of laminar flow and diffusion the H$_2$SO$_4$ concentration will develop a parabolic profile across the flow tube. Because of this radial gradient in H$_2$SO$_4$ the observed decay constant is a nonlinear function of the first-order wall loss rate and the pseudo first-order aerosol loss rate. To quantify the error introduced by our simplified analysis (which assumes that the observed rate constant is a linear sum of k_1 and k_d), we determined k_1 using the method of Brown [1978], modified for species detection in a central cross section of the laminar flow. With this method we calculated a cross-sectional sampling area based on the total flow through the sample inlet and the laminar flow velocity profile in the flow tube. Using this method, we found calculated values of first-order rate constant, k_1, within 2% of those values calculated by using the measured flow time from equation (1). The standard errors of the average value of α in both methods were the same. Here the radial gradients in the flow time and H$_2$SO$_4$ concentration across the sampled region were small enough that the observed rate constant, K, could be considered a linear sum of k_1 and k_d.

Error in the value of α will arise also from uncertainty in the SEMS measurements of the aerosol size distribution and calculated particle surface area. Most of this uncertainty is associated with accuracy in the pressure, flow rates, dilution of the sample gas, transmission of the particles through the DMA, the particle charging probabilities, and the inversion algorithm used to characterize the particle size distribution. We estimate the sum of the uncertainties in these parameters to be approximately 25% of the calculated particle surface area. The reported uncertainties in the average values of α for loss of H$_2$SO$_4$ onto NaCl and (NH$_4$)$_2$SO$_4$ particles is a sum of the 25% systematic error associated with the uncertainty in the aerosol surface area, a 3% error due to uncertainty in the H$_2$SO$_4$ diffusion coefficient, a 3% error in the flow time measurement, and twice the standard error (2σ).

Atmospheric Implications

Under the ambient conditions of the lower troposphere the composition and phase of submicron particles depend on the local sources of condensable gases and the relative humidity. The fine-mode particles in a remote marine environment are primarily aqueous solutions of sulfate, methyl sulfonate, and ammonium ions [Heubert et al., 1996; Savoie et al., 1993]. In addition to sulfate and ammonium ions, aerosols in continental air masses may contain nitrate ions and as much as

20-50% by mass organic molecules [Novakov and Penner, 1993; Saxena and Hildemann, 1996]. Also, gas phase sulfuric acid will be hydrated with one or more H$_2$O molecules almost entirely throughout the lower troposphere [Kulmala et al., 1991; Marti et al., 1997].

We can expect the uptake rate of H$_2$SO$_4$ onto particles to vary with the level of H$_2$SO$_4$ hydration and the particle composition. Although these experiments were conducted well below the deliquescence point of NaCl (75% RH) and (NH$_4$)$_2$SO$_4$ (80% RH), the aerosol surfaces likely had some H$_2$O coverage. Studies of H$_2$O adsorption isotherms on NaCl crystallites by Barraclough and Hall [1974] indicate that a NaCl crystallite surface has <0.1 to 0.5 monolayer of H$_2$O coverage over the corresponding 0.3-11% relative humidity range of the present experiments. Water adsorbed to the aerosol surface may provide a polar binding site and thereby enhance H$_2$SO$_4$ uptake. Also dependent on relative humidity is the percent hydration of H$_2$SO$_4$. At a relative humidity below 1%, H$_2$SO$_4$ is almost entirely unhydrated. However, at a 10% relative humidity, approximately 50% of the gas phase H$_2$SO$_4$ will be in a monohydrate form [Marti et al., 1997]. No appreciable trend in the mass accommodation coefficient with relative humidity was observed over the limited range of 0.3-11% RH. The small difference in the mass accommodation coefficients of H$_2$SO$_4$ for (NH$_4$)$_2$SO$_4$ and NaCl particle surfaces of the present study indicates either a similarity in the degree of H$_2$O coverage on these two salt particles or the fact that the uptake of H$_2$SO$_4$ onto the aerosols was relatively indifferent to H$_2$O on the salt surface. In the case of H$_2$SO$_4$ uptake onto a neutral salt the binding energy of H$_2$SO$_4$ appears strong enough that the acid readily adsorbed to the partially hydrated salt surface, and further enhancement of the uptake rate by additional water coverage may have little effect on an already high mass accommodation coefficient.

The uptake of H$_2$SO$_4$ onto wet, ambient aerosol droplets involves the adsorption and subsequent solvation of H$_2$SO$_4$ into the aqueous droplet. Here the energetics of solvation and hence reevaporation rate of H$_2$SO$_4$ depends on the Henrys law constant, which varies with the particle composition, pH, and temperature. The vapor pressure of H$_2$SO$_4$ above a mixed sulfate aerosol (i.e., a sulfuric acid/ammonium sulfate solution) was found to increase with the percent H$_2$SO$_4$ composition of the aerosol [Marti et al., 1997]. Thus the net uptake of H$_2$SO$_4$ is expected to decrease with particle acidity.

As is evident in the observed decrease in α for an aerosol coated with stearic acid, the initial adsorption of H$_2$SO$_4$ varies with the aerosol surface composition. As an oxidizing agent, H$_2$SO$_4$ may react chemically with organics present in the aerosol, leading to increased adsorption of H$_2$SO$_4$ onto aerosols. Our initial attempt at coating the aerosols with stearic acid involved solvating the stearic acid in ethanol or propanol. However, we found that these alcohols readily reacted with H$_2$SO$_4$ to form organic-sulfate clusters, which completely depleted the HSO$_4^-$ signal. This serendipitous discovery may indicate that H$_2$SO$_4$ reacts with atmospheric organics, either in the gas phase or in aerosol solutions.

The measured mass accommodation coefficients for NaCl and (NH$_4$)$_2$SO$_4$ aerosol may coincide well with the loss rate of H$_2$SO$_4$ onto neutral salt aerosols found in a remote marine environment. However, evidence from the reduced loss rate of H$_2$SO$_4$ onto an aerosol coated with an organic film and a previous experiment that found the H$_2$SO$_4$ vapor pressure above an aerosol to increase with aerosol acidity [Marti et al.,

1997] suggests that H_2SO_4 uptake onto aerosols varies broadly with the particle composition. Field measurements at a remote continental site that measured steady state H_2SO_4 production and loss rates found good agreement with their data, using a value of α of 0.5 and 1.0 [*Eisele and Tanner*, 1993; *Weber et al.*, 1997]. In these two field studies the aerosol likely had a mixed aqueous composition of SO_4^{2-}, NO_3^-, NH_4^+, inorganic metal and organic ions.

Conclusion

In this study we measured directly the H_2SO_4 loss rate onto submicron aerosols for three different aerosol substrates. The mass accommodation coefficients were calculated from the first-order rate constants and were found to be 0.73 ± 0.21 and 0.79 ± 0.23 for H_2SO_4 loss onto $(NH)_4SO_4$ and NaCl aerosols, respectively. The loss rate of H_2SO_4 onto a NaCl aerosol coated with stearic acid was lower than that of the salt aerosol with measured values of the mass accommodation coefficient of 0.31 and 0.19 for high and low stearic acid coverage, respectively.

The values of α are considerably higher than previous measurements of H_2SO_4 uptake onto aqueous H_2SO_4 droplets [*Van Dingenen and Raes*, 1991] but compare well with the value of $\alpha = 0.5$ to 1.0 deduced from the results of a field study of steady state production and loss rates of H_2SO_4 at a remote continental site [*Eisele and Tanner*, 1993; *Weber et al.*, 1997]. The higher values of α will result in higher calculated aerosol growth rates. In steady state model calculations of aerosol formation and growth, a higher aerosol growth rate would mean lower estimates of the gas phase H_2SO_4 concentration and consequently slower aerosol nucleation rates.

The uptake of H_2SO_4 was found to depend strongly on the aerosol composition, with a lower value of α reported for an aerosol with an organic coating. A similar reduction in α has been observed for uptake of NH_3 onto aerosol with an organic coating [*Däumer et al.*, 1992]. The variability in α with aerosol composition suggests that model evaluations of aerosol nucleation and growth need to consider the regional aerosol composition. In their model study, *Kerminen and Wexler* [1995] proposed using a value of α that decreases with increased aerosol size, because larger particles may have a higher organic composition and therefore a slower H_2SO_4 uptake. However, the chemical reactivity of H_2SO_4 with organics may affect their uptake onto aerosols such that α may vary with the specific organic compounds present in the aerosol.

Further studies of H_2SO_4 uptake onto aerosols indicative of the lower troposphere are needed to improve our understanding of aerosol growth and H_2SO_4 loss rates. Studies of the uptake rate of H_2SO_4 onto an aerosol surface of varying organic composition as well as aerosol pH, temperature, and relative humidity would enhance the ability of model calculations to predict aerosol formation and growth rates over a range of diverse atmospheres.

References

Ayers, G.P., R.W. Gillett, and J.L. Gras, On the vapor pressure of sulfuric acid, *Geophys. Res. Lett.*, 7, 433-436, 1980.

Barraclough, P.B., and P.G. Hall, Adsorption of water vapor by lithium fluoride, sodium fluoride and sodium chloride, *Surf. Sci.*, 46, 393, 1974.

Brown, R.L., Tubular flow reactors with first order kinetics, *J. Res. Natl. Bur. Stand. U.S.*, 83, 1-8, 1978.

Dahneke, B.E., Slip correction factors for nonspherical bodies, I, Introduction and continuum flow, *J. Aerosol Sci.*, 4, 139-145, 1973.

Däumer, B., R. Niessner, and D. Klockow, Laboratory studies of the influence of thin organic films on the neutralization reaction of H_2SO_4 aerosol with ammonia, *J. Aerosol Sci.*, 23, 315-325, 1992.

Eisele, F.L., and D.J.Tanner, Ion-assisted tropospheric OH measurements, *J. Geophys. Res.*, 96, 9295-9308, 1991.

Eisele, F.L., and D.J. Tanner, Measurement of the gas phase concentration of H_2SO_4 and methane sulfonic acid and estimates of H_2SO_4 production and loss in the atmosphere, *J. Geophys. Res.*, 98, 9001-9010, 1993.

Ewing, G.E., and S.J. Peters, Adsorption of water on NaCl, *Surf. Rev. Lett.*, in press, 1997.

Fuchs, N.A., and A.G. Sutugin, **Highly Dispersed Aerosols**, pp. 47-60, Butterworth-Heinemann, Newton, Mass.,1970.

Hagan, D. E., and D.J. Alofs, Linear inversion method to obtain aerosol size distributions from measurements with a differential mobility analyzer, *Aerosol Sci. Technol.*, 2, 465-475, 1983.

Heubert, B.J., L. Zhuang, S. Howell, K. Noone, and B. Noone, Sulfate, nitrate, methanesulfonate, chloride, ammonium, and sodium measurements from ship, island, and aircraft during the Atlantic Stratocumulus Transition Experiment/Marine Aerosol Gas Exchange, *J. Geophys. Res.*, 101, 4413-4423, 1996.

Kelly, W.P., and P.H. McMurry, Measurement of particle density by inertial classification of differential mobility analyzer-generated monodisperse aerosols, *Aerosol Sci. Technol.*, 17, 199, 1992.

Kerminen, V.M., and A.S. Wexler, Enhanced formation and development of sulfate particles due to marine boundary layer circulation, *J. Geophys. Res.*, 100, 23,051-23,062, 1995.

Kriedenweis, S.M., J. Penner, F. Yin, and J.H. Seinfeld, The effects of dimethylsulfide upon marine aerosol concentrations, *Atmos. Environ., Part A*, 25, 2501-2511, 1991.

Kulmala, M., M. Lazaridis, A. Laaksonen, and T. Vesala, Extended hydrates interaction model: Hydrate formation and the energetics of binary homogeneous nucleation, *J. Chem. Phys.*, 94, 7411-7413, 1991.

Kulmala, M., V.M. Kerminen, and A. Laaksonen, Simulations on the effect of sulfuric acid formation on atmospheric aerosol concentrations, *Atmos. Environ.*, 29, 377-382, 1995.

Lodge, J.P., and B.J. Tufts, An electron microscope study of sodium chloride particles as used in aerosol generation, *J. Colloid Sci.*, 10, 256, 1955.

Marti, J.J., A. Jefferson, X.P. Cai, C. Richert, P.H. McMurry, and F.L. Eisele, H_2SO_4 vapor pressure of sulfuric acid and ammonium sulfate solutions, *J. Geophys. Res.*, 102, 3725-3736, 1997.

Novakov, T., and J.E. Penner, Large contribution of organic aerosols to cloud-condensation nuclei concentrations, *Nature*, 365, 823-826, 1993.

Pandis, S.N., L.M. Russell, and J.H. Seinfeld, The relationship between DMS flux and CCN concentration in remote marine regions, *J. Geophys. Res.*, 99, 16,945-16,957, 1994.

Penner, J., T.M.L. Wigley, P. Jaumann, B.D. Santer, and K.E. Taylor, Anthropogenic aerosols and climate change: A method for calibrating forcing, in *Assessing Climate Change: The Story of the Model Evaluation*, Consortium for Clim. Assess. in press, 1997.

Roedel, W., Measurements of sulfuric acid saturation vapor pressure: Implications for aerosol formation by heteromolecular nucleation, *J. Aerosol Sci.*, 10, 375-386, 1979.

Savoie, D.L., J.M. Prospero, R.J. Larsen, F. Huang, M.A. Izaguirre, T. Huang, T.H. Snowdon, L. Custais, and C.G. Sanderson, Nitrogen and sulfur species in Antarctic aerosols at Mawson, Palmer Station, and Marsh (King George Island), *J. Atmos. Chem.*, 17, 95-122, 1993.

Saxena, P., and L.M. Hildemann, Water-soluble organics in atmospheric particles: A critical review of the literature and application of thermodynamics to identify candidate compounds, *J. Atmos. Chem.*, 24, 57-109, 1996.

Schwartz, S., The whitehouse effect. Shortwave radiative forcing of

climate by anthropogenic aerosols: An overview, *J. Aerosol Sci.*, *27*, 359-382, 1996.

Tanner, D.J., and F.L. Eisele, Present OH measurement limits and associated uncertainties, *J. Geophys. Res.*, *100*, 2883- 2892, 1995.

Tanner, D.J., A. Jefferson, and F.L. Eisele, Selected ion chemical ionization mass spectrometric measurement of OH, *J. Geophys. Res.*, *102*, 6415-6425, 1997.

Van Dingenen, R., and F. Raes, Determination of the condensation accommodation coefficient of sulfuric acid on water-sulfuric acid aerosol, *Aerosol Sci. Technol.*, *15*, 93-106, 1991.

Wang, S.C., and R.C. Flagan, Scanning electrical mobitity spectrometer, *Aerosol Sci. Technol.*, *13*, 230-240, 1990.

Weber, R.J., J.J. Marti, P.H. McMurry, F.L. Eisele, D.J. Tanner, and A.Jefferson, Measurements of new particle formation and ultrafine particle growth rates at a clean continental site, *J. Geophys. Res.*, *102*, 4375-4385, 1997.

Wigley, T.M.L., and S.C.B. Raper, Implications for climate and sea level of revised IPCC emissions scenarios, *Nature*, *357*, 293-300, 1992.

F.L. Eisele and A. Jefferson, Atmospheric Chemistry Division, National Center for Atmospheric Research, P.O. Box 3000, Boulder, CO 80307. (e-mail: ajeff@acd.ucar.edu)

J.J. Marti, Computational Physics, Inc., 2750 Prosperity Avenue, Fairfax, VA 22031-4323.

P.H. McMurry, Particle Technology Laboratory, Department of Mechanical Engineering, University of Minnesota, Minneapolis, MN 55455.

R.J. Weber, Environmental Sciences Laboratory, Brookhaven National Laboratory, U.S. Department of Energy, Upton, NY 11973.

P.J. Ziemann, Statewide Air Pollution Research Center and Department of Soil and Environmental Sciences, University of California, Riverside, CA 92521.